

Automatic navigation path detection method for tillage machines working on high crop stubble fields based on machine vision

Zhang Tian, Xia Junfang*, Wu Gang, Zhai Jianbo

(College of Engineering, Huazhong Agricultural University, Wuhan 430070, China)

Abstract: Due to the influence of complex working environment and artificial factors, it is easy to cause crop up over or less tillage problem when straw returning machine is working in paddy field. A new method for path detection suitable for rice, rape and wheat high crop stubble tilling environments was proposed. First the distribution characteristics of rice, rape and wheat high crop stubble images in paddy field based on RGB color model were analyzed, and rice, the color images of rape and wheat high crop stubble were converted into gray ones using custom factor combination $R+G-2B$; Then, the gray images of rice, rape and wheat high crop stubble were segmented from soil background by means of luminance mean texture descriptor; Next, the binary image through custom shear-binary-image algorithm was cut to remove big noise blobs in high crop stubble's tilled area; Finally, navigation path from navigation points by using the least square method was derived. The experimental results indicated that the navigation path detection algorithm was fast and effective to obtain navigation path in rice, rape and wheat high crop stubble tilling environments with up to 96.7% of segmentation accuracy within 0.6 s of processing time.

Keywords: high crop stubble, paddy field tilling, texture statistics, road navigation, vision navigation

DOI: 10.3965/j.ijabe.20140704.004

Citation: Zhang T, Xia J F, Wu G, Zhai J B. Automatic navigation path detection method for tillage machines working on high crop stubble fields based on machine vision. *Int J Agric & Biol Eng*, 2014; 7(4): 29–37.

1 Introduction

Due to the influence of complex work environment and artificial factors, it is easy to cause crop up over or less tillage problem when straw returning machine is working in paddy field. It results in dwindling the efficiency, increasing the energy consumption and

influencing next-stubble crop cultivation quality.

With the development of precision agriculture, precision navigation technology is an efficient approach to solve the problem. Navigation path identification is a fundamental technology to realize precise navigation, and machine vision provides the concept and technologies needed for path identification, with many advantages such as extensive use, multi-function and cost effectiveness^[1-6]. Those researches mainly concentrated on drought crop path recognition aspects, such as row crops, ridge line, furrow lines and boundary between tilled area and non-tilled area^[7-10] at present. In drought crop-row detection respect, Wang Xiaoyan et al.^[11] put forward a kind of navigation path detection method to recognize standing maize stubble rows on conservation tillage farm, and the experiments with a large number of field images showed that this method had a good adaptability when implement worked under small deflection, within 15 degrees, instead of large. In drought crop ridge line recognition, Zhang Zhibin et

Received date: 2014-02-23 **Accepted date:** 2014-08-10

Biographies: **Zhang Tian**, Postgraduate, research interests: agricultural intelligent detection using image processing. Tel: +86-13307145898, Email: xfzhangtian@163.com. **Wu Gang**, Postgraduate, research interests: agricultural intelligent detection using image processing. Tel: +86-13554061540, Email: kgdmqj.2008@yahoo.com.cn. **Zhai Jianbo**, PhD student, research interests: modern agricultural equipment and information technology, Tel: +86-18086496518, Email: zhaibo123456@163.com.

***Corresponding author:** **Xia Junfang**, PhD, Professor, research interests: modern agricultural equipment design and measurement and control. Tel: +86-18694048763, Email: xjf@mail.hzau.edu.cn.

al.^[12,13] reported a new approach to detect straight line, in which the subsets of the pixels, image matrix and prior knowledge of ridge width were employed to estimate the center points of crop rows. The algorithm could effectively avoid the interference from weeds during extracting trajectory center points of ridge line. In term of furrow line in dry field, Zhao Ying et al.^[14] analyzed the different color features of tilled area and non-tilled area. The red component chosen as segmentation index by the authors was sufficient for extracting alternate point group along furrow line slope direction. Besides, for boundary recognition between tilled area and non-tilled area, Wu Gang et al.^[15] focused on wheat harvest boundary and used the improved Hough transform method to detect object line, Zhang Chengtao et al.^[16] proposed a new path recognition algorithm of visual navigation based on improved smoothness texture feature on the basis of Wu Gang's study in order to meet combine harvester's demand of real-time and robustness requirement to some extent. Compared with natural navigation path in dry field, the natural navigation path in paddy field, formed once crop stubble was returned to soil, was more complex and less clear because there were some crop stubble unburied in the soil, some mud with different shapes, high reflective water and bubbles floating on the water, which made its detection more difficult. At present, navigation path recognition of high crop stubble returned boundary in paddy field has not yet been investigated.

The main objective of this study was to propose and experimentally verify a new method for detecting navigation path in high crop stubble paddy fields. The steps for navigation path detection method are outlined below: firstly, rice, rape and wheat high crop stubble

were separated from soil background by means of luminance mean texture descriptor. Secondly, custom shear-binary-image method was used to cut the binary images to remove big noise blobs in tilled area. Thirdly, navigation candidate points were extracted based on cut binary images with the help of row scan. Finally, navigation path was obtained through least square method fitting navigation candidate points.

2 Material and methods

2.1 Image acquisition

Influenced by southern farming system and cultivation patterns, there are usually abundant crop straw residues such as rice, rape and wheat stubble in agricultural fields^[17,18]. The BenQ DCC420 type digital camera was installed at front right position of the tractor, aligned with machine's right work boundary. Its height apart from above ground was about 1 m, angle of depression was about 15°, and depth of focus was about 5 m. Three typical high crop stubbles, which are rice, rape and wheat high crop stubble, were taken in rice core test area of modern agricultural science and technology in Huazhong Agricultural University and rice - wheat planting region in Huanghu new village, Tuanfeng County, Hubei Province respectively. The images mainly included high crop residues tilled area and non-tilled area. Figures 1a-1c show three kinds of typical high crop stubble images captured when they were being tilled (hereafter field image of high crop stubble or field image for short). The crop strains are rice, rape and wheat from left to right respectively. The image size was 480 by 640 pixels in JPEG format. Matlab image processing module is used to analyze the images.



Figure 1 Field images of rice, rape and wheat high crop stubble

2.2 Navigation path detection

2.2.1 Navigation path detection algorithm

The field images of rice, rape and wheat high crop stubble obtained in paddy field under natural environment mainly includes high crop residues tilled area and non-tilled area. The boundary between tilled area and non-tilled area, namely, navigation path of straw returning machine, is object line in this paper.

Navigation path detection algorithm process is illustrated in Figure 2, and described below:

- 1) To acquire grayscale images of rice, rape and wheat high crop stubble using custom combination color factor R+G-2B;
- 2) To separate rice, rape and wheat high crop stubble from soil background by means of luminance mean texture descriptor and obtain high crop stubble binary image;
- 3) To utilize custom shear-binary-image method to remove big noise blobs in high crop stubble's tilled area;
- 4) To extract navigation candidate points based on high crop stubble cut binary images;
- 5) To obtain navigation path using least square method.

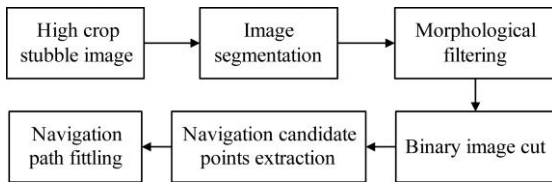


Figure 2 Navigation path detection algorithm flow chart

2.2.2 Image graying method

Since type of high crop stubble is different in paddy field, general grayscale method does not work. This research puts forward the innovative combination color factor R+G-2B based on statistics of color factors of rice, rape and wheat high crop stubble's tilled and non-tilled area, which was measured and analyzed with the AOI (Area of Interest) testing tool under RGB color model.

2.2.3 Image segmentation method

The texture feature of local area where high crop stubbles corresponded is fairly clear but that of soil is disorganized^[19,20]. It provides a pathway for detecting navigation path through extracting texture feature of rice, rape and wheat high crop stubble's tilled area and non-tilled area.

Description methods of regional texture feature include statistical method, structural method and spectral method. Considering the complexity and real-time performance of algorithm, statistical method based on gray histogram statistics was selected as texture feature extraction method and its computation formula is:^[21]

$$\text{Mean value } m = \sum_{i=0}^{L-1} z_i p(z_i) \quad (1)$$

$$\text{Standard deviation } \sigma = \sqrt{\sum_{i=0}^{L-1} (z_i - m)^2 p(z_i)} \quad (2)$$

$$\text{Smoothness value } R = 1 - \frac{1}{(1 + \sigma^2)} \quad (3)$$

$$\text{The third order moment } \mu_2 = \sum_{i=0}^{L-1} (z_i - m)^2 p(z_i) \quad (4)$$

$$\text{Consistency } U = \sum_{i=0}^{L-1} p(z_i)^2 \quad (5)$$

$$\text{Entropy } e = - \sum_{i=0}^{L-1} p(z_i) \log_2 p(z_i) \quad (6)$$

where, $i=0,1,\dots,L-1$, L is the number of gray levels; z_i is a random variable used for describing intensity of area, and $p(z_i)$ is gray level histogram of area.

Then, a better texture descriptor suitable for this paper was selected based on texture statistic of each small window of rice, rape and wheat high crop stubble images using Matlab software program.

2.2.4 Denoising method

Due to the influence of complex work environment^[22] and the bad performance of tillage implement work, it is inevitable to observe rice, rape and wheat high crop residue in tilled area because of not being entirely covered by soil. It means that there must be some white points or area namely target points or area, in tilled area of the binary image. Morphological filtering can work on the small and independent white spots, but for larger white area, common morphology used for removing noise is far from effective.

Aiming at large target spots in tilled area, shear-binary-image algorithm was presented innovatively in this paper, and its algorithm flowchart is as follows: firstly, we obtained binary image through image preprocessing; then, we computed accumulative pixel values L_j of the binary image in vertical direction according to formula (7) and average A of the maximum

and minimum value of accumulative pixel values L_j according to formula (8); then, we selected the corresponding column number of $0.1 \times A$ and $1.8 \times A$ accumulative pixel values as shear boundaries; finally, we retained pixel values of some region that middle section of shear boundaries corresponded to and set other regions zero.

$$L_j = \sum_{i=1}^M f(i, j) \quad (7)$$

$$A = \frac{1}{2} (\max(L_j) + \min(L_j)) \quad (8)$$

where, M and N are the number of rows and columns of the binary image, $0 < j \leq N$ and $f(i, j)$ is the pixel value of row i and column j in image.

2.2.5 Navigation candidate points extraction method

The two principal areas of shear binary image are tilled area and non-tilled area. Where, high crop stubble's non-tilled area turns into white (pixel value was 1) while its tilled area becomes black (pixel value was 0). According to this feature, the possible arisen location of navigation candidate points could be estimated. The concrete practices are as follows:

Store coordinates of navigation alternate points in (X_m, Y_m) (m is the number of alternate points). The cropping binary image was divided into m equal segments, and each part contains s rows. We obtained the last non zero pixel point in every row by scanning the cropping binary image from top to bottom, and then put the ordinate in array b_j ($0 \leq j \leq N$, j is the number of column, N is the total number of columns). The exact location (x_i, y_i) of the i -th alternate point could be calculated as follows:

$$\begin{cases} x_i = \frac{s}{2} + (i-1) \times s \\ y_i = \frac{1}{s} \sum_{j=(i-1) \times s + 1}^{i \times s} b_j \end{cases} \quad (9)$$

2.2.6 Navigation path fitting method

Currently, the main navigation line detection algorithms are Hough transform^[23-26] and the least square method^[27-29]. Though Hough transform has been widely used because of its robustness, there are disadvantages of large storage space, large amount of calculation, time-consuming and "false line" and so on^[30]. From the

perspective of a given dataset with the minimum mean square error (MSE), the potential benefits of the least square method includes simple calculation formula, high speed of calculation and higher precision^[31], and it is more suitable for this test. Regression formula of the least square method is as follows:

A given dataset is $\{(x_i, y_i) | 1 \leq i \leq N\}$, and ascertained linear regression equation is $y = ax + b$. If error index is

$$E = \sum_{i=1}^N (ax_i + b - y_i)^2 \quad (10)$$

When the mean square error (MSE) is the least, straight line parameters a and b satisfied

$$\frac{\partial E}{\partial a} = 0, \quad \frac{\partial E}{\partial b} = 0 \quad (11)$$

That is

$$\begin{aligned} \sum_{i=1}^N 2(ax_i + b - y_i)x_i &= 0, \\ \sum_{i=1}^N 2(ax_i + b - y_i) &= 0 \end{aligned} \quad (12)$$

Rewrite formula (12), and assume

$$\begin{aligned} S_x &= \sum_{i=1}^N x_i, S_y = \sum_{i=1}^N y_i, \\ S_{xx} &= \sum_{i=1}^N x_i^2, S_{xy} = \sum_{i=1}^N x_i y_i \end{aligned} \quad , \text{ then}$$

$$\begin{cases} S_{xx}a + S_x b - S_{xy} = 0 \\ S_x a + N b - S_y = 0 \end{cases} \quad (13)$$

Regression line equation can be obtained by solving system of equations:

$$y = \frac{S_x S_y - N S_{xy}}{S_x^2 - N S_{xx}} x + \frac{S_{xy} S_x - S_{xx} S_y}{S_x^2 - N S_{xx}} \quad (14)$$

3 Results and discussion

3.1 Gray factor analysis

With the purpose of finding an appropriate factor that could transform all or almost all rice, rape and wheat high crop residue images into gray images, twenty in each high crop residue images (rice, rape and wheat) were selected randomly, and their tilled and non-tilled area were measured and analyzed with the AOI (Area of Interest) testing tool under RGB color model. The data were derived from the average of the same color feature factor under the same crop stubble. Table 1 presents the statistical results.

Table 1 Statistical mean values of color feature factors R, G and B

Color factors	Rice stubble non-tilled area	Rice stubble tilled area	Rape stubble non-tilled area	Rape stubble tilled area	Wheat stubble non-tilled area	Wheat stubble tilled area
R	144	166	120	187	159	122
G	132	156	121	171	147	112
B	78	147	71	158	101	97

Table 1 shows that there was no unified rule which could hold for any of color component under the same crop between tilled and non-tilled area. In particular, the values of all color components of rice and rape stubble in non-tilled area were significantly lower than those of tilled area, which were significantly higher for wheat crop stubble except for B component. However, no matter which type of crop stubble, the same crop stubble’s R and G color components were higher than its B color component with 50 - 70 gray level in non-tilled area, and 10 - 30 gray level in tilled area. Based on the above analysis, and regarding reduction of feature recognition error and enhancement of image grayscale contrast, color factor combination $R + G - 2B$ was chosen to transform color image into gray image to have a better target segmentation performance.

3.2 Image segmentation factor analysis

Since the extraction of texture describer is all based on image area’s grayscale histogram statistics, it is particularly important to ensure statistic window size. Considering the robustness, real time and accuracy of the algorithm, the better size of the region window should be

as large as possible and meanwhile less than the minimum size of local area where rice, rape and wheat high crop residue matched. Combined with actual shape and posture of different crop residues presented in the images, the better window size was intended to be 12 by 2 (column by row) pixels.

The statistics about six texture descriptors were acquired by testing tilled and non-tilled area of 20 in each high crop residue images (rice, rape and wheat). Table 2 shows the average statistics of the same descriptor with the same crop series.

As seen in Table 2, differences of the values of intensity mean values, standard deviation and smoothness among non-tilled areas of different crop stubbles were not as significant as that between tilled area and non-tilled area, which provided a guarantee for segmenting field images. The third order moment mirrored the skew of the gray histogram, and consistency and entropy reflected the homogeneity of the gray histogram. They were closely related to the shooting location and angle besides residues type and density, so all three could not be regarded as the main indexes in image segmentation.

Table 2 Statistical mean values of texture descriptors of different crop stubble’s non-tilled and tilled regions

Area	Texture descriptors					
	Intensity mean value	Standard deviation	Smoothness	Third moment	Consistency	Entropy
Rice stubble non-tilled area	187.0247	25.9962	0.0166	-0.2377	0.1888	3.2386
Rape stubble non-tilled area	218.2917	20.0076	0.0079	0.0430	0.1730	3.3977
Wheat stubble non-tilled area	236.4486	16.3564	0.0160	-0.5942	0.7992	0.6909
Stubble tilled area	83.59	8.0370	0.0040	0.0396	0.1918	2.9342

Taking field image of rice stubble as example (if without a special statement, field image means that of rice stubble hereafter), the process of determining optimal threshold in image segmentation is as follows:

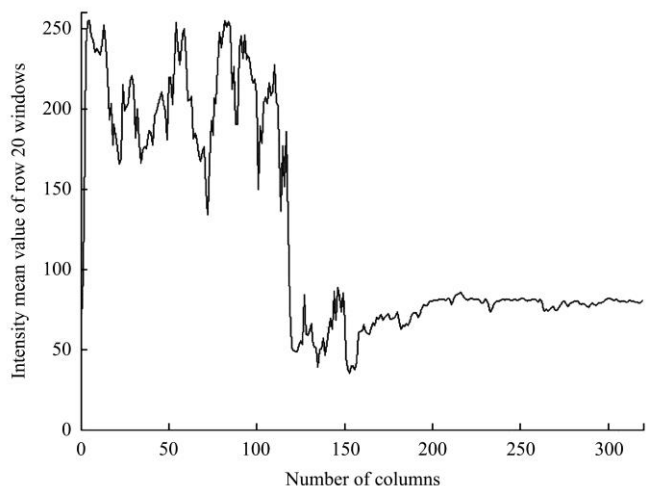
- 1) To set an empty matrix Q, the size was the same as the number of regions which was generated after field image was divided by window, marked as 40 by 320;
- 2) To calculate three texture descriptors (intensity mean value, standard deviation and smoothness) of each

region, and then store the results in corresponding position of Q. For example, if (i, j) was the region’s row and column coordinates, the result as a whole was stored in Q in i row and j column;

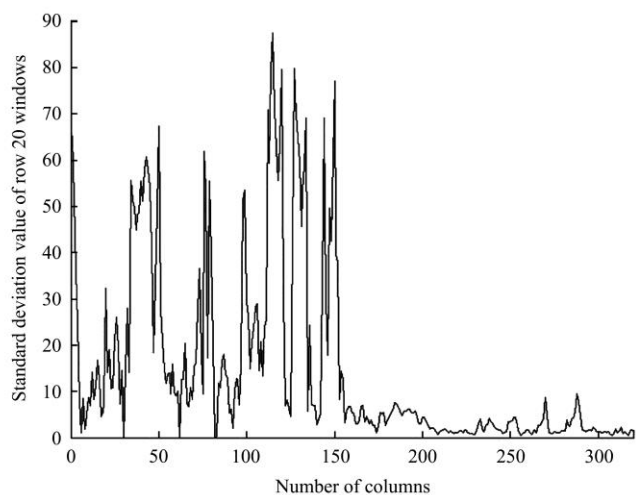
- 3) To determine optimal texture descriptor used for image segmentation. Selected a row of matrix Q randomly first, then described the data of the row in the term of curve, and finally picked out the best texture descriptor in consideration of difficulty when threshold

was selected and error when image was segmented;

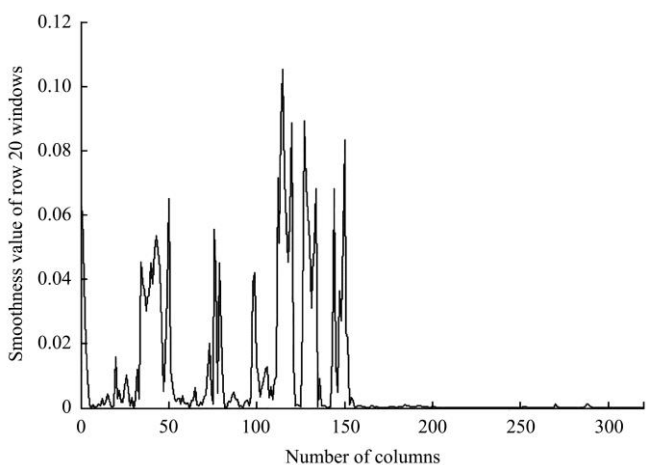
4) To assign the optimal texture descriptor in accordance with homologous curve.



a. Intensity mean value



b. Standard deviation



c. Relative smoothness value

Figure 3 Texture descriptor information of rice straw image

Setting the threshold 100 and segmenting field image of rice stubble (Figure 1a), the result is presented as Figure 4.

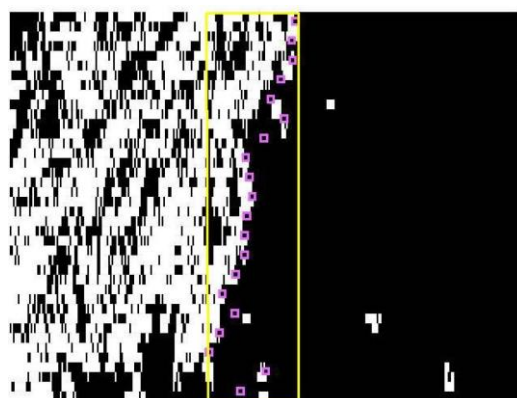


Figure 4 Result of rice stubble image segmentation

To further validate the point, 30 in each high crop residue images (rice, rape and wheat), totally 90, selected randomly were processed as above. Set the segmentation correct standard: the dividing line between tilled and non-tilled area was sharp, and the extraction for navigation path feature point was not affected by target points or blocks in tilled area. Table 3 shows the test results.

Table 3 Target segmentation results under different texture descriptors

Texture descriptors	The number of false segmentation	The number of correct segmentation	Correct segmentation rate
Intensity mean value	3	87	96.7%
Standard deviation	9	81	90%
Smoothness	12	78	86.7%

The test results proved that image segmentation based on intensity mean texture descriptor has stronger robustness with the segmentation accuracy of 96.7% and indicated that the boundary information between tilled and non-tilled area could be effectively extracted.

3.3 Navigation candidate points extraction analysis

The area inside yellow box in Figure 4 is the result of shear binary image using shear-binary-image method put forward innovatively in this paper. It is very obvious that the area almost does not contain large target spots in tilled area, that is to say, shear-binary-image method could effectively remove large noise spots in tilled area. Rose red squares in Figure 4 are the navigation candidate points extracted by the above algorithm. To show the navigation candidate points clear, the rose red squares are in bold. It could be seen that the navigation candidate points, extracted based on shear binary image, could truly reflect the trend of

navigation path, and were scarcely affected on white spots in tilled area. That was to say, the algorithm had strong anti-interference.

3.4 Navigation path analysis

Figures 5a-5c were the results of processing Figure 1a-1c used the navigation path detection algorithm. In

image coordinate system in pixels(image row as abscissa, image column as ordinate), the slopes of the three straight lines in Figures 5a-5c were -3.8, -1.6 and -5 respectively, and the intercepts were 1 378.8, 881.3 and 1 964.9 respectively.

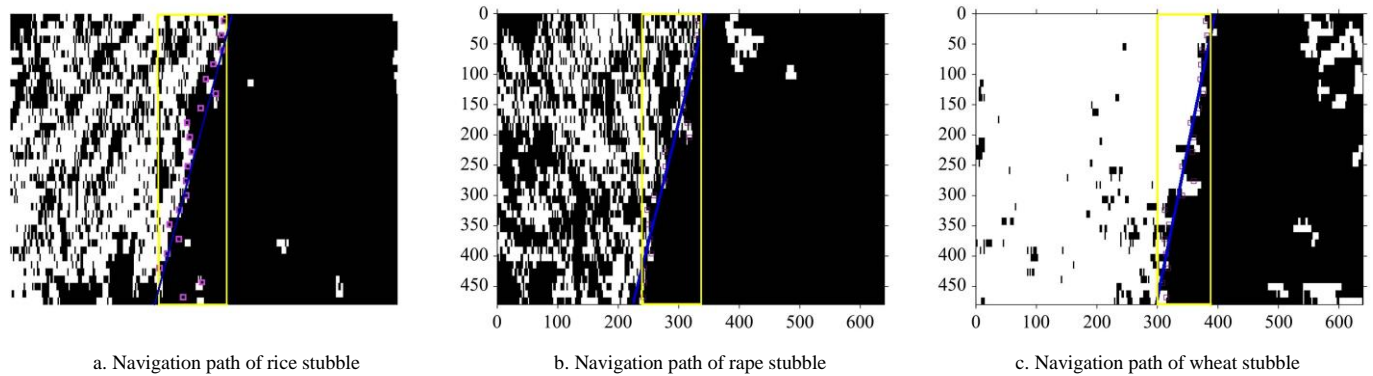


Figure 5 Path detection results of different high crop stubble field images

To measure the effectiveness of the navigation path detection algorithm, 20 images for each high crop stubble field images were tested. The results showed that almost all the navigation paths overlapped with the corresponding high crop stubble tilled and non-tilled boundaries. The candidate points that extracted from shearing binary image could effectively reflect the tilled and non-tilled boundary information and were nearly not affected by white spots in tilled area. That was, the

algorithm was strong to resist interference. Results show that processing time is less than 0.6 s, therefore, the least square method for fitting navigation path increased detection speed and high precision, hence it was suitable for real time processing.

Figures 6a-6c were rice, rape and wheat high crop stubble field images with big slope tillage boundaries from left to right, captured when tractor was keeping close to tillage boundary. Figures 6d-6f were the

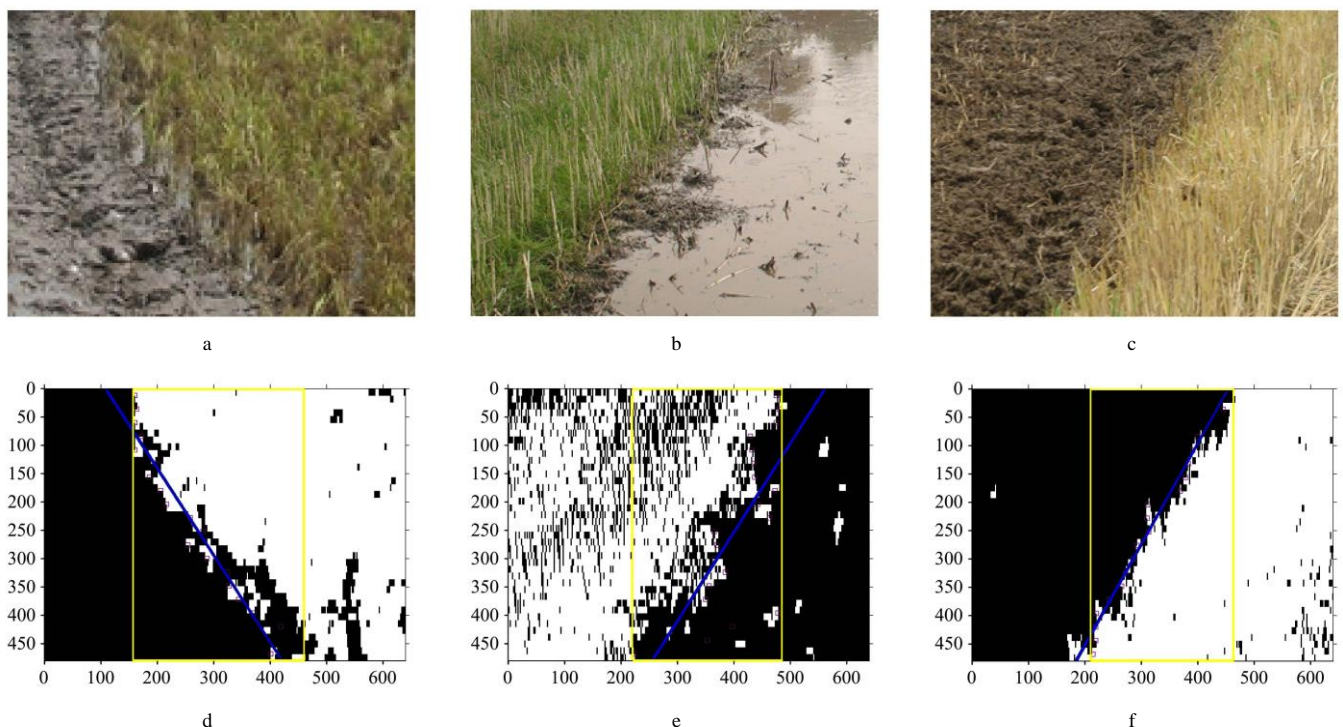


Figure 6 Path detection results of different high crop stubble field images in big shooting degree of skewness

corresponding detection results. The experiment showed that the algorithm was well adaptive to larger slope navigation path image.

4 Conclusions

In order to improve the degree of automation and intelligentization of straw returning machine and solve the over and less tillage problem, navigation path detection algorithms of rice, rape and wheat high crop stubble were studied. Findings are as follows:

1) Based on intensity mean value texture descriptor segmenting field image, it could effectively separate object area from soil background.

2) Shearing binary image before extracting navigation path candidate points was an effective method to dwindle the influence of the white spots in background area, and the navigation path candidate points could truly reflect the trend of navigation path, and be well robust. The use of the least square method for fitting navigation path has fast detection speed and high precision. Therefore it could meet the need of real-time processing.

3) The experimental results proved that, navigation paths, derived by navigation path detection algorithm under different crop species (rice, rape and wheat), all efficiently reflected the tillage boundary. The algorithm was adaptable.

Acknowledgements

This work was financially supported by the Special Fund for Agro-scientific Research in the Public Interest (No. 201203059) and the Natural Science Foundation of China (No. 51275196). We greatly appreciate the support.

[References]

- [1] Ding Y C, Wang S M. Vision navigation control system for combine harvester. *Transactions of the CSAM*, 2010; 41(5): 137–142. (In Chinese with English abstract)
- [2] Li J, Chen J P, Xu C S, Wang M L, Wang J E. Path tracking of intelligent vehicle based on dynamic image threshold. *Transactions of the CSAM*, 2013; 44(4): 39–44. (In Chinese with English abstract)
- [3] Gottschalk R, Burgos-Artizzu X P, Ribeiro A, Marin G B. Real-time image processing for the guidance of a small agricultural field inspection vehicle. *International Journal of Intelligent Systems Technologies and Applications*, 2010; 8(1): 434–443.
- [4] Subramanian V, Burks T F, Arroyo A A. Development of machine vision and laser radar based autonomous vehicle guidance systems for citrus grove navigation. *Computers and Electronics in Agriculture*, 2006; 53(2): 130–143.
- [5] Finlayson G D, Hordley S D, Lu C, Drew M S. On the removal of shadows from images. *IEEE Transactions on Pattern Analysis and Machine Intelligence*, 2006; 28(1): 59–68.
- [6] Leemans V, Destain M F. Application of the Hough transform for seed row localisation using machine vision. *Biosystems Engineering*, 2006; 94(3): 325–336.
- [7] Zhao B, Zhu Z X, Song Z H, Xie B, Mao E R. Path recognition method for vision navigation of agricultural vehicle. *Journal of Jiangsu University*, 2007; 28(6): 482–486.
- [8] Ding Y C, Wang S M, Chen D. Navigation line detection arithmetic based on image rotation and projection. *Transactions of the CSAM*, 2009; 40(8): 155–160. (In Chinese with English abstract)
- [9] Zhao B, Mao E R, Mao W H, Zhang X C, Song Z H. Path recognition for vision navigation system of agricultural vehicle in weed environment. *Transactions of the CSAM*, 2009; 40: 183–186. (In Chinese with English abstract)
- [10] Ding Y C, Liao Q X, Huang H D, Duan H B, Chen H, Chen X K. Large curvature path detection for combine harvester based on vision navigation. *Transactions of the CSAM*, 2011; 42: 123–127. (In Chinese with English abstract)
- [11] Wang X Y, Chen Y, Chen B Q, Duan H B. Detection of stubble row and inter-row line for computer vision guidance in no-till field. *Transactions of the CSAM*, 2009; 40(6): 158–163. (In Chinese with English abstract)
- [12] Zhang Z B, Luo X W, Li Q, Wang Z M, Zhao Z X. New algorithm for machine vision navigation of farm machine based on well-ordered set and crop row structure. *Transactions of the CSAE*, 2007; 23(7): 122–126. (In Chinese with English abstract)
- [13] Zhang Z B, Luo X W, Wang Z M. A new algorithm for identifying the crop row image based on subsets and nearest neighbor rule. *Journal of Image and Graphics*, 2007; 12(11): 2048–2051.
- [14] Zhao Y, Chen B Q, Wang S M, Dai F Y. Fast detection of furrows based on machine vision on autonomous mobile robot. *Transactions of the CSAM*, 2006; 37(4): 83–86. (In Chinese with English abstract)
- [15] Wu G, Tan Y, Zheng Y J, Wang S M. Walking goal line detection based on improved Hough transform on harvesting robot. *Transactions of the CSAM*, 2010; 41(2): 176–179. (in

- Chinese with English abstract)
- [16] Zhang C T, Tan Y, Wu G, Wang S M. Visual navigation system path recognition algorithm based on DaVinci platform for combine harvester. *Transactions of the CSAM*, 2012; 43(10): 271–276. (In Chinese with English abstract)
- [17] Zhang G Z, Xu Q C, Xia J F, Zhou Y. Design of IGMC-70 ship type rotary tillage. *Transactions of the CSAM*, 2008; 39(10): 214–217. (In Chinese with English abstract)
- [18] Xia J F, Zhang G Z, Xu Q C, Huang H D, Zhou Y. Research on the mechanized technology of rotary tillage and stubble-mulch for paddy field under multiple rice cropping system. *Journal of Huazhong Agricultural University*, 2008; 27(2): 331–334. (In Chinese with English abstract)
- [19] Zhou P, Wang Y M, Zhao Y, Xu Y F. Fast cut-uncut segmentation of textural natural image for autonomous navigation. *Transactions of the CSAM*, 2004; 35(4): 97–101. (In Chinese with English abstract)
- [20] Zhang F M. Study on algorithms of field road detection and stereovision-based guidance algorithm for a field vehicle. Hangzhou: Zhejiang University, 2006.
- [21] Rafael C G, Richard E W, Steven L E. Digital image processing. MATLAB. Ruan Qiuqi translation. Beijing: Publishing House of Electronics Industry, 2005; 9.
- [22] Guo S Y, Zhai W J, Tang Q, Zhu Y L. Combining the Hough transform and an improved least squares method for line detection. *Computer Science*, 2012; 39(4): 196–200.
- [23] Rovira-Ma's F, Zhang Q, Reid J F, Will J D. Hough transform-based vision algorithm for crop row detection of an automated agricultural vehicle. *Journal of Automobile Engineering*, 2005; 219(8): 999–1010.
- [24] Rao H H, Ji C Y. Crop-row detection using Hough transform based on connected component labeling. *Transactions of the CSAE*, 2007; 23(3): 146–150. (In Chinese with English abstract)
- [25] Wu G, Tan Y, Zheng Y J, Wang S M. Walking goal line detection based on improved Hough transform on harvesting robot. *Transactions of the CSAM*, 2010; 41(2): 176–179. (In Chinese with English abstract)
- [26] Xie Z H, Ji C Y, Guo X Q, Ren S G. An object detection method for quasi-circular fruits based on improved Hough transform. *Transactions of the CSAE*, 2010; 26(7): 157–162. (In Chinese with English abstract)
- [27] Si Y S, Jiang G Q, Liu G, Gao R, Liu Z X. Early stage crop rows detection based on least square method. *Transactions of the CSAM*, 2010; 41(7): 163–167. (In Chinese with English abstract)
- [28] Yang R J, Liu R, Xu K X. Detection of urea in milk using two-dimensional correlation spectroscopy and partial least square method. *Transactions of the CSAE*, 2012; 28(6): 259–263. (In Chinese with English abstract)
- [29] Song H Y, Qin G, Han X P, Liu H Q. Soil classification based on near infrared reflectance spectroscopy and orthogonal signal correction-partial least square. *Transactions of the CSAE*, 2012; 28(7): 168–171. (In Chinese with English abstract)
- [30] Wang X Z, Han X, Mao H P, Liu F. Navigation line detection of tomato ridges in greenhouse based on least square method. *Transactions of the CSAM*, 2012; 43(6): 161–166. (In Chinese with English abstract)
- [31] Feng J, Liu G, Si Y S, Wang S M, He B, Ren W. Algorithm based on image processing technology to generate navigation directrix in orchard. *Transactions of the CSAM*, 2012; 43(7): 185–189. (In Chinese with English abstract)